A conductometric enzymatic methanol sensor based on polystyrene - PAMAM dendritic polymer electrospun nanofibers

Pouyan Razmshoar, Fatma Besbes, Anis Madaci, Rym Mlika, S. Hajir Bahrami, Mohammad Rabiee, Marie Martin, Abdelhamid Errachid, Nicole Jaffrezic-Renault

A conductometric enzymatic methanol sensor based on polystyrene - PAMAM dendritic polymer electrospun nanofibers

Pouyan Razmshoar[1,2], Fatma Besbes[2,3], Anis Madaci[2], Rym Mlika[3], S. Hajir Bahrami[1], Mohammad Rabiee[4], Marie Martin[2], Abdelhamid Errachid[2], Nicole Jaffrezic-Renault[2*]

1. Textile Engineering Department, Amirkabir University of Technology (Tehran Polytechnic), Tehran, Iran

2. University of Lyon, Institute of Analytical Sciences, UMR 5280, CNRS, F-69100, Villeurbanne, France

3. University of Monastir, Laboratory of Interfaces and Advanced Materials, Faculty of Science of Monastir, 5019 Monastir, Tunisia

4. Biomedical Engineering Department, Amirkabir University of Technology (Tehran Polytechnic), Tehran, Iran

Corresponding authors: Nicole Jaffrezic-Renault, nicole.jaffrezic@univ-lyon1.fr

Abstract:

Methanol (MeOH) is a solvent and cleaning agent used in industry, but it is poisonous when ingested. The recommended release threshold for MeOH vapor is 200 ppm. We present a novel sensitive micro-conductometric MeOH biosensor created by grafting alcohol oxidase (AOX) onto electrospun polystyrene-poly(amidoamine) dendritic polymer blend nanofibers (PS-PAMAM-ESNFs) on interdigitated electrodes (IDEs). The analytical performance of the MeOH microsensor was evaluated using gaseous MeOH, ethanol, and acetone samples collected from the headspace above aqueous solution with known concentration. The sensor's response time (t_{Res}) fluctuates from 13 s to 35 s from lower to higher concentrations. The conductometric sensor has a sensitivity of 150.53 µS.cm-1 (v/v) for MeOH and a detection limit of 100 ppm in the gas phase. The MeOH sensor is 7.3 times less sensitive to ethanol and 136.8 times less sensitive to acetone. The sensor was verified for detecting MeOH in commercial rubbing alcohol samples.

Keywords: Micro-conductometric sensor; Alcohol oxidase; Methanol sensor; Nanofibers; Dendrimer; Rubbing alcohol.

1. Introduction

Methanol, the simplest alcohol, is harmless on its own, but its metabolites formic acid and formate are very hazardous after ingestion [1,2]. It is well known that consuming MeOH may harm the neurological and circulatory systems permanently, leading to blindness, organ failure, or even death. It can be found in alcoholic drinks made by distillation or spontaneous fermentation. Blindness cases have been documented following the ingestion of as little as 4 mL of MeOH. It is often stated that 100 mL of consumed MeOH is the least deadly dosage [1]. MeOH is often employed as a cleaning agent and solvent in industry, and it is an alternate energy carrier to hydrogen [3]. For repeated exposure during the working day without experiencing serious health consequences, INRS (the French National Institute of Research and Security) proposes a released threshold for MeOH vapor concentration of 200 ppm for an 8 h's exposure. It is thus necessary to create assays and sensors that are sensitive, reasonably priced, and easy to use for industrial laboratories, suppliers, and end users. MeOH has been identified using a variety of methods, such as gas chromatography [4], Fourier transform infrared spectrometry [5], Raman spectroscopy [6], and surface plasmon resonance [7]. These methods are not suited for routine usage because of their limitations, which include high costs and the requirement for skilled personnel. To address the issue, a gas sensor approach has been used to detect MeOH or other volatile organic chemicals (VOCs).

Numerous sensors are based on semiconducting metal oxides. For the detection of MeOH, nanostructured metal oxides such as SnO_2, ZnO, In_2O_3, and α-Fe_2O_3 show excellent sensitivity as well as ferrite-type perovskites [8]. The main drawbacks of these nanomaterials are their high working temperature and their rather poor specificity.

Taking advantage of the enzyme selectivity, enzyme-based sensors were used as a ''bio-sniffer'' for the detection of methanol. Alcohol oxidase (AOX) is an oligomeric FAD-dependent enzyme that oxidizes MeOH by accepting electrons from molecules of oxygen (O_2) and generating formaldehyde and hydrogen peroxide (Eq. (1)). Since O_2 has a significant oxidizing effect, MeOH is irreversibly oxidized by AOX:

$$CH_3OH + O_2 \xrightarrow{AOX} HCOH + H_2O_2 \quad (1)$$

Following the reaction, optical or electrochemical detections can be used to measure either the decrease of O_2 or the increase of H_2O_2 concentration. Until recently, all electrochemical transducers presented have been amperometric or voltametric [9].

MeOH in exhaled breath, for non-invasive assessment of intestinal flora, was detected through fluorometry, using a cascade reaction with two enzymes, AOX from *Pichia pastoris* and formaldehyde dehydrogenase from *Pseudomonas sp.*. The dynamic range of the MeOH sensor was 0.32–20 ppm [10].

Another AOX-based biosensor was developed for the detection of MeOH in the aqueous phase through photoelectrochemistry with AOX from *Hansenula sp*. immobilized in the presence of cysteine-stabilized cadmium sulphide quantum dots that photocatalyze oxidation of 1-thioglycerol. The detection limit of MeOH was found to be 0.01 ppb. No interference with ethanol was observed [11].

An alcohol biosensor was obtained by the immobilization in polyvinyl alcohol of a bienzymatic system (AOX from *Hansenula sp.*+ catalase from bovine liver) on a microconductometric transducer. The biosensor provided a lower detection limit for MeOH (0.5 µM, 16 ppb), compared to that of ethanol, in aqueous solutions [9].

In this work, a microconductometric transduction was chosen for the detection of MeOH in the headspace above aqueous solutions through its oxidation by AOX from *Pichia pastoris*. In comparison to other AOX, the active site cavity of this AOX is significantly reduced in size, which could explain the observed preference for MeOH as substrate [12].

Polymeric nanofibers have been investigated for application in the construction of sensors due to their unique properties, such as their large surface area, facile surface functionalization, and interconnected porosity, which aid in improved interaction with the surrounding medium and access to the desired analyte [13]. Researchers have preserved enzyme stability by immobilizing them on the surface of nanofibers [14-16]. In this work, we employed PS-PAMAM dendritic polymer blend nanofibers to immobilize AOX. PS is well-known for its distinct properties, such as good shape stability in aqueous media and non-swelling, as well as its low cost and excellent spinnability [17]. On the other hand, PS has been altered using PAMAM, a highly branched polymer, and active amine groups have been

designed on the surface of ESNFs to stabilize the AOX. Dendrimers are the perfect matrix for stabilizing biomolecules because of their distinctive properties, including their spherical shape, size controllability, high surface groups, hydrophilicity, and excellent physical and chemical stability. These characteristics boost the sensitivity, selectivity, stability, and reusability of biosensors as well as their capacity to capture target molecules [18]. For instance, the researchers developed an amperometric biosensor based on immobilizing AOX on PAMAM and utilized it to identify ethanol based on the consumption of dissolved oxygen concentration. The sensor's limit of detection (LOD) was 0.016 mM, with a detection range of 0.025 to 1.0 mM. The stability studies of bioanalytical characteristics preservation revealed 67% of the initial sensitivity after 1 month at 4°C [19]. To form a strong covalent link between the AOX and the fiber surface, glutaraldehyde coupling chemistry was employed to form a bond between the PAMAM dendritic polymer groups and the amine groups on the AOX's outer surface. The conductometric sensor, which incorporates an IDEs coated with a thin layer of PS-PAMAM ESNFs on which AOX is immobilized, is shown step by step in Scheme 1. The volatile alcohols are measured directly in the headspace above the aqueous solutions using conductometry. The analytical performance of the novel MeOH sensor was determined. For its validation, the determination of the MeOH content in rubbing alcohol was performed.

Scheme 1.

2.Materials and Methods

2.1 Reagents and solutions

The reagents and solutions were fully addressed in the supplemental material.

2.2 Technology of fabrication of the micro conductometric chips

A chrome-on-glass mask was designed for the production of interdigitated gold microelectrodes with a width of 20 µm and an interelectrode distance of 20 µm. The electrical tracks were 500 µm wide. The lithography and deposition steps are carried out on 4-inch (Borosilicate) glass substrates, 1mm thick with two polished sides. The photosensitive resin used for the process was AZ 5214 E resin, which is a

reversible resin but, in this case, used in positive mode (the exposed parts were left during the development). In order to improve the adhesion of the resin to the wafer, a primer was used, which was spread with the same program as the resin. The spreading of the primer and of the resin were consecutive. The assembly was then annealed at 120°C on a hot plate for 120 s. The thickness of the resin deposited on the wafer was approximately 1.4 μm. The UV KUB 2 system, working with an LED carpet, was used for insolation. The maximum power of the KUB UV was 23.2 mW/cm² (100%). It was critical that the Cr/glass mask and resin mask made good contact. The insolation parameters were 70% of the maximum power for 10 s. The development was carried out in the AZ 726 MIF developer for 1 min with a slight manual agitation. The reaction was stopped by immersing the wafer in a large volume of DI water, then the wafer was rinsed with DI water, and finally it was dried under a dry air flow. Before carrying out the deposition by electron gun, the wafers were cleaned by plasma using the RIE NGP 80 frame. The process conditions were: 55 sccm O2, 100 mTorr, 70 W (13.56 MHz RF generator), and duration 120 s. The metal deposition was carried out in an EVA 300 vacuum frame. The substrates were fixed to an uncooled rotating sample holder. The high-voltage generator was set at 7.4 kV. A thickness of 20 nm of titanium was deposited, and then a thickness of 150 nm of gold was deposited. At the end of the deposition, lift-off was carried out; the samples were immersed in an acetone bath under ultrasound for 30 min. To remove the last residues, a new plasma cleaning was carried out under the same conditions as before, but for a period of 10 min. The chips were then cut into pairs of electrodes using the DISCO saw. A flow chart of the fabrication process is presented in Figure 1. An excellent reproducibility from one microelectrode to another and excellent gold adhesion was obtained. The glass wafer covered with interdigitated electrodes cut in pairs, and supported on a blue film is presented in Figure S1.

The chips were detached from the blue film and rinsed with acetone and ethanol to remove any contaminants that would hinder the encapsulating resin from adhering to the surface. The connections were covered with the encapsulation resin, which was made by combining two EPOTECH polymers (50/50 by weight) to designate the measuring area. The micro-conductometric chips were 5×30 mm in size and consisted of two identical gold interdigitated electrodes.

Figure 1

2.3 Preparation of the methanol sensor

2.3.1 Preparation of PS-PAMAM ESNFs based micro conductometric chips

To create a 20 wt.% PS-PAMAM electrospinning solution, 0.14 g of PAMAM and 0.26 g of PS granules were each individually dissolved in 1 mL of N,N-dimethylformamide (DMF) and agitated overnight at room temperature (RT). Then, the PAMAM was gradually and carefully added to the PS, and the mixture was stirred for an additional 4 h. Following this step, the homogeneous PS-PAMAM solution was used immediately for electrospinning. The solution loaded into a 1 mL syringe was fed to the nozzle head (a laser-cut needle, 22 gauges) with the help of an electrospinning pump through a polytetrafluoroethylene (PTFE) tube (vertical electrospinning device, Spraybase®, Ireland). The electrospinning parameters were 20 kV for the voltage, 0.25 mL/h for the feed rate, and 20 cm for the working distance, and they were optimized in the prior investigation to produce beadless nanofibers with a uniform diameter [20]. PS-PAMAM nanofibers were electrospun on each micro conductometric chip for 1 min by placing the interdigitated electrodes under the vertical spinning device in order to obtain the greatest degree of uniformity across the electrodes in terms of the thickness and quantity of ESNFs deposited. The micro conductometric chips containing nanofibers were stored at RT until the subsequent stages of sensor manufacturing.

2.3.2 AOX Immobilization

The enzyme immobilization on the biosensor surface was carried out by a method of protein cross-linking in saturated glutaraldehyde (GA) vapor, as previously optimized [9]. Typically, the PS-PAMAM ESNFs based sensor was placed in saturated GA vapor for 45 min. In parallel, BSA (2,8 mg/mL) was first dissolved in 10 mM PBS (pH = 7). The solution was mixed with AOX enzyme (2 mg/mL). The mixture containing AOX and BSA was deposited dropwise on the sensitive surface of the PS-PAMAM ESNFs based sensor (working sensor) and then kept dried at 4°C in the refrigerator until further usage. The reference sensor was functionalized only with BSA. After one night int the fridge, it was possible to used the sensor.

2.4 Instrumentation

2.4.1 Physicochemical Characterizations

The Characterizations were fully addressed in the supplemental material.

2.4.2 Conductometric measurements

Conductometric VOC detection was accomplished by applying an alternating voltage (10 mV amplitude, 10 kHz frequency) generated by a very low-frequency wave-form generator to each pair of interdigitated electrodes (working sensor and reference sensor). These parameters enabled reductions in faradaic processes, double-layer charging, and concentration polarization at the microelectrode surface. These parameters had previously been optimized in KCl solutions. A conductometer VigiZMeter was used to record the sensors' differential output signal (COVARIANS Gif-sur-Yvette, France). The working/reference sensor pair was placed in the headspace over a liquid phase in a cylindrical container to accomplish these measurements. The conductance (G) measurement was recorded versus time throughout the insertion of the sensor pair into the headspace and its withdrawal from the headspace.

2.5. Preparation of gas samples

Gaseous MeOH, ethanol, and acetone samples were collected from the headspace above aqueous solutions of known concentrations between 0 and 100%.

The concentrations of MeOH and ethanol in the gas phase above the aqueous solutions are determined using the Henry's law constants of the given analytes in water, according the equation reported by Sander [21], at 25°C.

$$k_H^0 = c_a / p_g \qquad \text{(eq. 1)}$$

Where k_H^0 refers to Henry's law constants for the standard condition; $[k_H^0]$= M/atm. c_a is the concentration of a species in the aqueous phase; $[c_a]$=M, and p_g is the partial pressure of that species in the gas phase; $[p_g]$ =atm.

For the listed solvents, MeOH, ethanol, and acetone, Henry's law constants value are rspectively 2.2×10^2 M/atm, 2×10^2 M/atm, and 0.2×10^2 M/atm at 25°C [22].

The calculated equilibrium gas-phase concentrations of MeOH, ethanol, and acetone above the aqueous phase are shown in Tables S1, S2, and S3.

3. Results and discussion

3.1. Characterization of the PS-PAMAM ESNFs mats

The homogeneity in the diameter of the nanofibers has a significant impact on the performance of nanofiber-based sensors, including the repeatability of the results and reproducibility of the sensor. An FESEM microscope was used to analyze the nanofibers' morphology. According to the photograph in Figure 2 (A), PS-PAMAM ESNFs have a uniform diameter and a smooth surface without any beads. The main reason for this is the presence of PAMAM in the electrospinning solution, which increases the electrical conductivity of the electrospinning solution and the surface charge of the jet during flight, as a result of which the electrospinning jet is subjected to more instabilities and causes the nanofiber diameter to decrease. The uniformity of the diameter, both along the length of a single fiber and in the average diameter of the fibers, is confirmed by the histogram of Figure 2 (B)'s narrow diameter distribution, which will result in repeatability and reproducibility for the desired sensor. The branching polymer's active sites and the average diameter of 200 nm will give a large amount of accessible surface area for enzymes, leading to a significantly higher level of stability of the enzyme on the fiber surface.

Figure 2.

The FTIR test was used to evaluate the chemical structure of PS-PAMAM ESNFs and to validate the presence of PAMAM amine groups in the structure and surface of nanofibers. In all spectra (Figurec3), the characteristic peaks of PS at 696 cm^{-1} and 755 cm^{-1} associated with C−H out-of-plane bending vibration, 1451 cm^{-1} and 1492 cm^{-1} related to CH_2 bending vibrations, 1600 cm^{-1} linked to C=C stretching vibrations, 2846 cm^{-1}, 2920 cm^{-1}, and 3080-3024 cm^{-1} related to aromatic C−H

stretching vibration absorption, and the presence of CH_2 were present. Characteristic bands of PAMAM are also found in the spectra of PS-PAMAM ESNFs at 1372 cm^{-1}, 1551 cm^{-1}, and 1645 cm^{-1}, corresponding to C−N stretch of amide III, N−H bending and C−N stretch of amide II band, and C=O of amide I band, respectively. Furthermore, the band at 3268 cm^{-1} is associated with N−H stretching vibration (Figure 3. (A)). These bands show that PAMAM is intercalated in the PS fiber structure without any interaction with PS because the FTIR bands of amide I, amide II and amide III remain at the same positions as those of the pristine PAMAM grafted on the surface of PS fibers [13,23]. The spectra of GA-PS-PAMAM ESNFs (Figure 3. (B)) shows two additional peaks at 1644 cm^{-1} and 1715 cm^{-1} that are associated to GA. Moreover, the peak at 1674 cm^{-1} is connected to the C=N group, confirming the covalent link between the NH_2 of PAMAM and the C=O of GA [20]. The peak at 1715 cm^{-1} associated to GA has diminished owing to binding between the AOX and GA after immobilization of AOX on the surface of PS-PAMAM ESNFs based micro conductometric chip [24,25] (Figure 3. (C)).

Figure 3.

3.2 Analytical performance of the micro-conductometric methanol sensor

Conductometric detection of numerous VOCs (MeOH, ethanol, acetone, chloroform, and toluene) was carried out in the gaseous phase above pure liquid compounds at 25°C in order to assess the discrimination capacity of an AOX/PS-PAMAM ESNFs-based sensor, as shown in Figure 4. The conductivity signal increased dramatically when exposed to the headspace of MeOH. The nanofibers' large accessible surface area, along with the designed surface chemistry supplied by the PAMAM, permitted very high immobilization of the AOX on the electrode surface, resulting in very high sensor sensitivity. In comparison to ethanol and acetone, the sensor has shown significantly higher sensitivity to MeOH. It should be emphasized that the sensor showed no response following exposure to toluene and chloroform. This demonstrates the proposed sensor's remarkable sensitivity to MeOH.

Figure 4.

The response time (t_{Res}) is defined as the amount of time needed to achieve 90% of the total change in conductance following introduction into the headspace, and the recovery time (t_{Rec}) is defined as the amount of time needed to achieve 10% of the total change in conductance following withdrawal from the headspace.

As shown in the diagram in Figure S2, the t_{Res} of the AOX/PS-PAMAM ESNFs-based conductometric sensor was from 13 s to 35 s from lower concentrations of MeOH to its higher concentrations. The t_{Rec} was from 6 s to 10 s from lower concentrations to higher concentrations.

Figure S2.

The detection of different gas-phase concentrations of MeOH is presented in Figure 5. When the MeOH concentration was zero and the sensor was exposed to pure water, the conductivity that was recorded corresponded to 100% humidity at that time and was 22 µS/cm. The observed signal at 9v/v% MeOH concentration was 1100 µS/cm; the contribution of 89v/v% humidity is then 1.8% of this signal, which is within the experimental error range for this concentration. This low contribution of humidity is due to the differential measuring method between the working sensor with AOX and the reference sensor with BSA. The non specific signal for water is then cancelled.

Figure 5.

The calibration curves of gas-phase concentrations of MeOH, ethanol, and acetone are presented in Figure S3. The MeOH sensor presents the best linearity of $R^2 = 0.9707$, and the best sensitivity of 150.53 $\mu S.cm^{-1}(v/v)$. The MeOH sensor has a detection limit of 100 ppm, calculated from the formula 3s/S where s is the is the standard deviation of 3 different blanks and S is the slope of the calibration plot. The sensitivities for ethanol and acetone are 20.4

273 µS/cm(v/v) and 1.1 µS/cm(v/v), respectively, showing that the MeOH sensor presents a 7.3 times
274 higher sensitivity than ethanol and 136.8 times higher than acetone. The relative standard deviation of
275 the measurements is 2%. The inter-sensor reproducibility is 5%. The shelf life of the MeOH sensor is
276 one month when continuously used.

277 **Figure S3.**

278

279 A lot of MeOH sensors have been fabricated, mainly based on semi-conducting compounds (SnO_2,
280 TiO_2, CdS) and on Ni phthalocyanine (Table 1). Meanwhile, this is the first time that an AOX/PS-
281 PAMAM ESNFs based sensor is used for the conductometric detection of MeOH. Compared to the
282 other conductometric MeOH sensors, the prepared MeOH sensor works at room temperature, presents
283 a short response time, but it has a rather high detection limit.

284

285 **Table 1.**

286

287 ***3.3 Detection of alcohol content in rubbing alcohol through the gas phase***

288 Rubbing alcohol, a product made from 95% MeOH, is used as a liquid on barbecues or fireplaces or as
289 an antifreeze solvent. In addition, if used at home, it is a powerful cleaner for stubborn dirt, polishing
290 numerous surfaces, and removing stains.

291 After the detection of MeOH in the headspace of absolute MeOH and of an 80% MeOH /water
292 mixture, the detection of MeOH in the headspace of a commercial rubbing alcohol "Alcohol de
293 QUEMAR" was conducted as presented in Figure S4.

294 The conductivity found for the commercial sample was 1282 µS/cm. This value corresponds to 10.31
295 ± 0.23 v/v%. The corresponding concentration in the liquid phase of the rubbing alcohol is 23.60 ±
296 1.30 M. This corresponds to 91.17 ± 1.5 v/v%, which is in good agreement with the supplier's figure
297 of 95%.

298

299 **Figure S4**.

4. Conclusion

A highly sensitive MeOH sensor based on AOX/PAMAM dendritic-polystyrene polymer blend nanofibers was successfully developed in this study. The sensitivity for MeOH is 7.3 times higher than for ethanol. The sensor is selective, sensitive, has a short response time, and has a shelf life of one month. The detection limit is lower than the recommended threshold for MeOH vapor concentration for exposed workers.

Acknowledgements

Campus France is acknowledged for the financial support through PHC Maghreb EMBISALIM. CNRS is acknowledged for the financial support through IRP NARES. Region Auvergne Rhone-Alpes is acknowledged through EMBAI project. P.R. would like to gratefully acknowledge the Ministry of Science, Research, and Technology of Iran for providing the scholarship.

326

327

328

Figure and Table Captions

Scheme 1. Stages of the fabrication of the ESF-based conductometric sensor

Figure1. Flow chart of the technology of fabrication of the micro conductometric chips

Figure 2. (A) FESEM image and (B) the diameter distribution of PS-PAMAM ESNFs.

Figure 3. FTIR spectra of (A) PS-PAMAM, (B) GA-PS-PAMAM, and (C) AOX/PS-PAMAM ESNFs.

Figure 4. Detection of gas-phase concentrations above the pure liquid phase of MeOH, acetone, chloroform, ethanol, and toluene.

Figure 5. Detection of gas-phase concentration above different MeOH /water solutions with the MeOH sensor.

Table 1. Comparison of the analytical performances of conductometric MeOH sensors based on different materials.

References

[1] J.A. Kruse, Methanol poisoning, Intensive Care Med. 18 (1992) 391–397.

[2] K.E. Hovda, O.H. Hunderi, A. Tafjord, O. Dunlop, N. Rudberg, D. Jacobsen, Methanol outbreak in Norway 2002–2004: epidemiology, clinical features and prognostic signs, J. Intern. Med. 258 (2005) 181–190.

[3] F. Schorn, J.L. Breuer, R.C. Samsun, T. Schnorbus, B. Heuser, R. Peters, D. Stolten, Methanol as a renewable energy carrier: An assessment of production and transportation costs for selected global locations, Adv. Appl. Energy. 3 (2021) 100050.

[4] J.A. Joseph, S. Akkermans, J.F.M. Van Impe, Processing Method for the Quantification of Methanol and Ethanol from Bioreactor Samples Using Gas Chromatography–Flame Ionization Detection, Acs Omega. 7 (2022) 24121–24133.

[5] K. Sharma, S.P. Sharma, S. Lahiri, Novel method for identification and quantification of methanol and ethanol in alcoholic beverages by gas chromatography-fourier transform infrared spectroscopy and horizontal attenuated total reflectancefourier transform infrared spectroscopy, J. AOAC Int. 92 (2009) 518–526.

[6] P. Maksimov, A. Laari, V. Ruuskanen, T. Koiranen, J. Ahola, Gas phase methanol synthesis with Raman spectroscopy for gas composition monitoring, RSC Adv. 10 (2020) 23690–23701.

[7] S. Kumar, G. Sharma, V. Singh, Modelling of surface plasmon resonance sensor for detection of mass concentration of ethanol and methanol in a binary mixture, Infrared Phys. Technol. 67 (2014) 190–196.

[8] A. Mirzaei, S.G. Leonardi, G. Neri, Detection of hazardous volatile organic compounds (VOCs) by metal oxide nanostructures-based gas sensors: A review, Ceram. Int. 42 (2016) 15119–15141.

[9] M. Hnaien, F. Lagarde, N. Jaffrezic-Renault, A rapid and sensitive alcohol oxidase/catalase conductometric biosensor for alcohol determination, Talanta. 81 (2010) 222–227.

[10] K. Toma, K. Iwasaki, G. Zhang, K. Iitani, T. Arakawa, Y. Iwasaki, K. Mitsubayashi, Biochemical methanol gas sensor (MeOH bio-sniffer) for non-invasive assessment of intestinal

flora from breath methanol, Sensors. 21 (2021) 4897.

[11] J. Barroso, B. Diez-Buitrago, L. Saa, M. Möller, N. Briz, V. Pavlov, Specific bioanalytical optical and photoelectrochemical assays for detection of methanol in alcoholic beverages, Biosens. Bioelectron. 101 (2018) 116–122.

[12] C. Koch, P. Neumann, O. Valerius, I. Feussner, R. Ficner, Crystal structure of alcohol oxidase from Pichia pastoris, PLoS One. 11 (2016) e0149846.

[13] P. Razmshoar, S.H. Bahrami, M. Rabiee, I.A.M. Frias, M. Hangouet, M. Martin, F. Bessueille, A. Errachid, N. Jaffrezic-Renault, An impedimetric immunosensor based on PAMAM decorated electrospun polystyrene fibers for detection of interleukin-10 cytokine, J. Electroanal. Chem. 926 (2022) 116953.

[14] Z.G. Wang, L.S. Wan, Z.M. Liu, X.J. Huang, Z.K. Xu, Enzyme immobilization on electrospun polymer nanofibers: An overview, J. Mol. Catal. B Enzym. 56 (2009) 189–195. https://doi.org/10.1016/j.molcatb.2008.05.005.

[15] W.-C. Huang, W. Wang, C. Xue, X. Mao, Effective enzyme immobilization onto a magnetic chitin nanofiber composite, ACS Sustain. Chem. Eng. 6 (2018) 8118–8124.

[16] X. Su, J. Ren, X. Meng, X. Ren, F. Tang, A novel platform for enhanced biosensing based on the synergy effects of electrospun polymer nanofibers and graphene oxides, Analyst. 138 (2013) 1459–1466.

[17] B. Rezaei, A.M. Shoushtari, M. Rabiee, L. Uzun, A.P.F. Turner, W. Cheung Mak, Multifactorial modeling and optimization of solution and electrospinning parameters to generate superfine polystyrene nanofibers, Adv. Polym. Technol. 37 (2018) 2743–2755. https://doi.org/10.1002/adv.21947.

[18] J. Satija, V.V.R. Sai, S. Mukherji, Dendrimers in biosensors: Concept and applications, J. Mater. Chem. 21 (2011) 14367–14386. https://doi.org/10.1039/c1jm10527b.

[19] M. Akin, M. Yuksel, C. Geyik, D. Odaci, A. Bluma, T. Höpfner, S. Beutel, T. Scheper, S. Timur, Alcohol biosensing by polyamidoamine (PAMAM)/cysteamine/alcohol oxidase- modified gold electrode, Biotechnol. Prog. 26 (2010) 896–906.

[20] P. Razmshoar, S.H. Bahrami, M. Rabiee, M. Hangouet, M. Martin, G. Raffin, A. Errachid, N.

Jaffrezic-Renault, Novel platform based on polystyrene electrospun nanofibrous mats doped with PAMAM dendritic polymer for enhanced immunosensing, Appl. Surf. Sci. (2021) 152221.

[21] R. Sander, Compilation of Henry's law constants for inorganic and organic species of potential importance in environmental chemistry, (1999).

[22] J.R. Snider, G.A. Dawson, Tropospheric light alcohols, carbonyls, and acetonitrile: Concentrations in the southwestern United States and Henry's law data, J. Geophys. Res. Atmos. 90 (1985) 3797–3805.

[23] P. Razmshoar, S. Hajir Bahrami, M. Rabiee, M. Hangouet, M. Martin, A. Errachid, N. Jaffrezic-Renault, A novel electrochemical immunosensor for ultrasensitive detection of tumor necrosis factor α based on polystyrene - PAMAM dendritic polymer blend nanofibers, Microchem. J. 175 (2022) 107206. https://doi.org/10.1016/j.microc.2022.107206.

[24] C.H. Chuang, H.P. Wu, Y.W. Huang, C.H. Chen, Enhancing of intensity of fluorescence by DEP manipulations of polyaniline-coated Al2O3 nanoparticles for immunosensing, Biosens. Bioelectron. 48 (2013) 158–164. https://doi.org/10.1016/j.bios.2013.03.064.

[25] M. Mahmoudifard, M. Soleimani, M. Vossoughi, Ammonia plasma-treated electrospun polyacrylonitryle nanofibrous membrane: The robust substrate for protein immobilization through glutaraldhyde coupling chemistry for biosensor application, Sci. Rep. 7 (2017) 1–14. https://doi.org/10.1038/s41598-017-10040-7.

[26] K. Phasuksom, W. Prissanaroon-Ouajai, A. Sirivat, A highly responsive methanol sensor based on graphene oxide/polyindole composites, RSC Adv. 10 (2020) 15206–15220.

[27] J. van den Broek, S. Abegg, S.E. Pratsinis, A.T. Güntner, Highly selective detection of methanol over ethanol by a handheld gas sensor, Nat. Commun. 10 (2019) 4220.

[28] P. Bindra, A. Hazra, Selective detection of organic vapors using TiO2 nanotubes based single sensor at room temperature, Sensors Actuators B Chem. 290 (2019) 684–690.

[29] C.-F. Fong, C.-L. Dai, C.-C. Wu, Fabrication and characterization of a micro methanol sensor using the CMOS-MEMS technique, Sensors. 15 (2015) 27047–27059.

[30] I. Musa, G. Raffin, M. Hangouet, M. Martin, A. Alcacer, N. Zine, F. Bellagambi, N.

Jaffrezic- Renault, A. Errachid, Development of a Chitosan/Nickel Phthalocyanine Composite Based Conductometric Micro- sensor for Methanol Detection, Electroanalysis. 34 (2022) 1338–1347.

[31] I. Musa, G. Raffin, M. Hangouet, M. Martin, J. Bausells, N. Zine, F. Bellagambi, N. Jaffrezic-Renault, A. Errachid, Electrospun PVC-nickel phthalocyanine composite nanofiber based conductometric methanol microsensor, Microchem. J. 182 (2022) 107899.

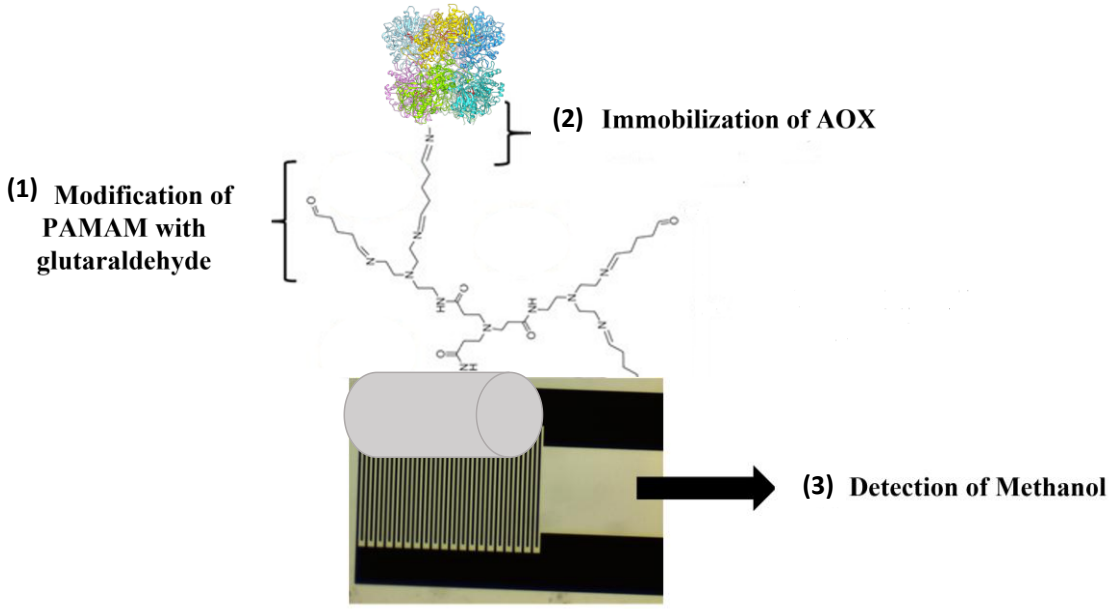

Scheme 1. Stages of the fabrication of the ESF-based conductometric sensor

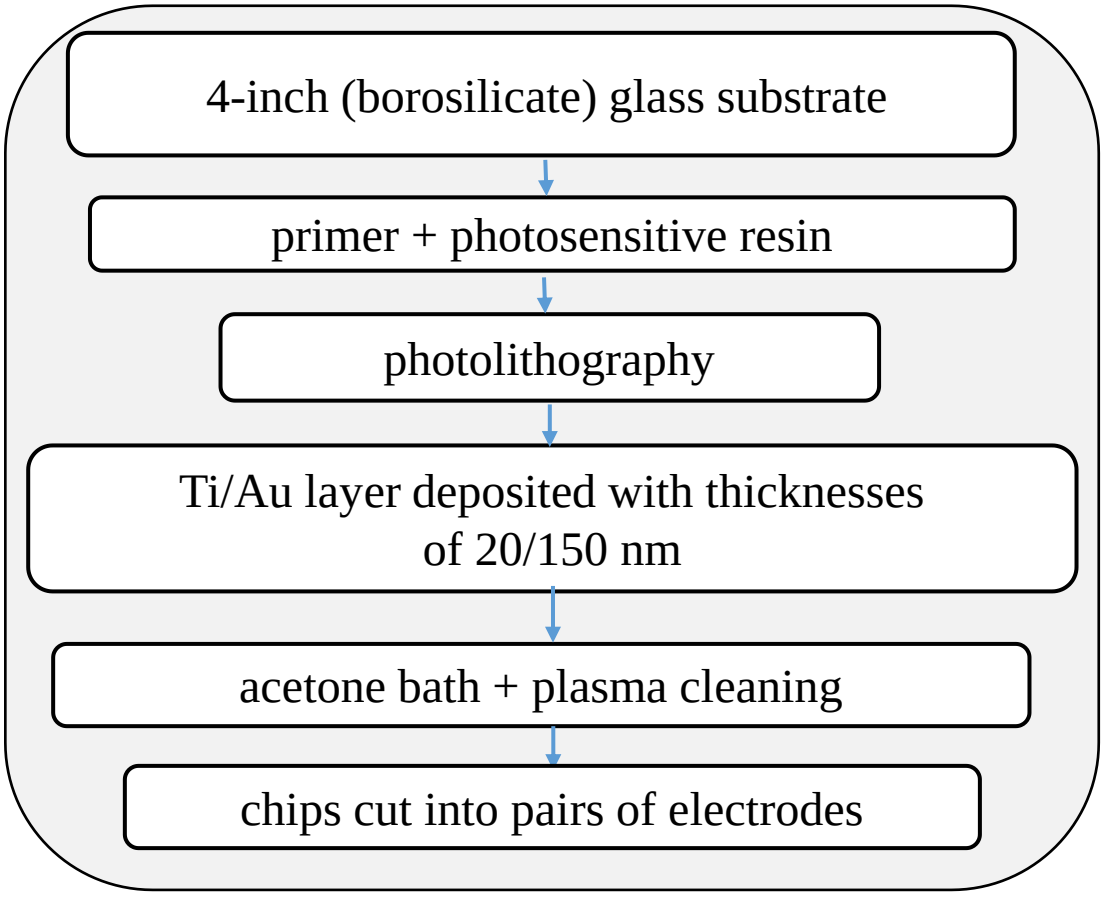

Figure1. Flow chart of the technology of fabrication of the micro conductometric chips

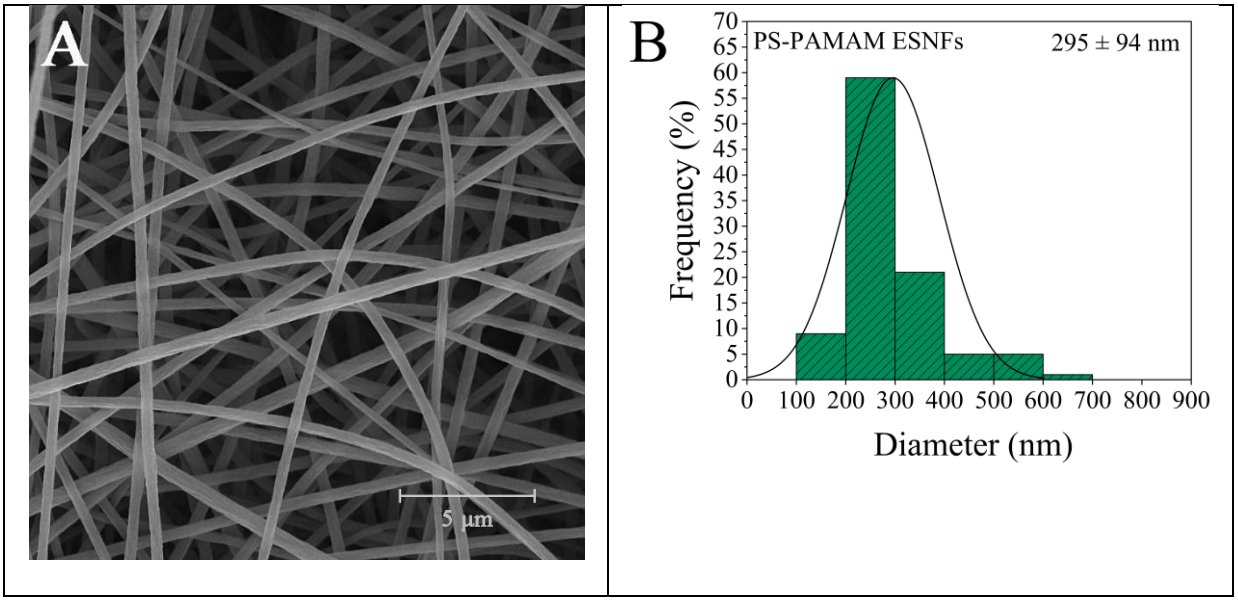

Figure 2. (A) FESEM image and (B) the diameter distribution of PS-PAMAM ESNFs.

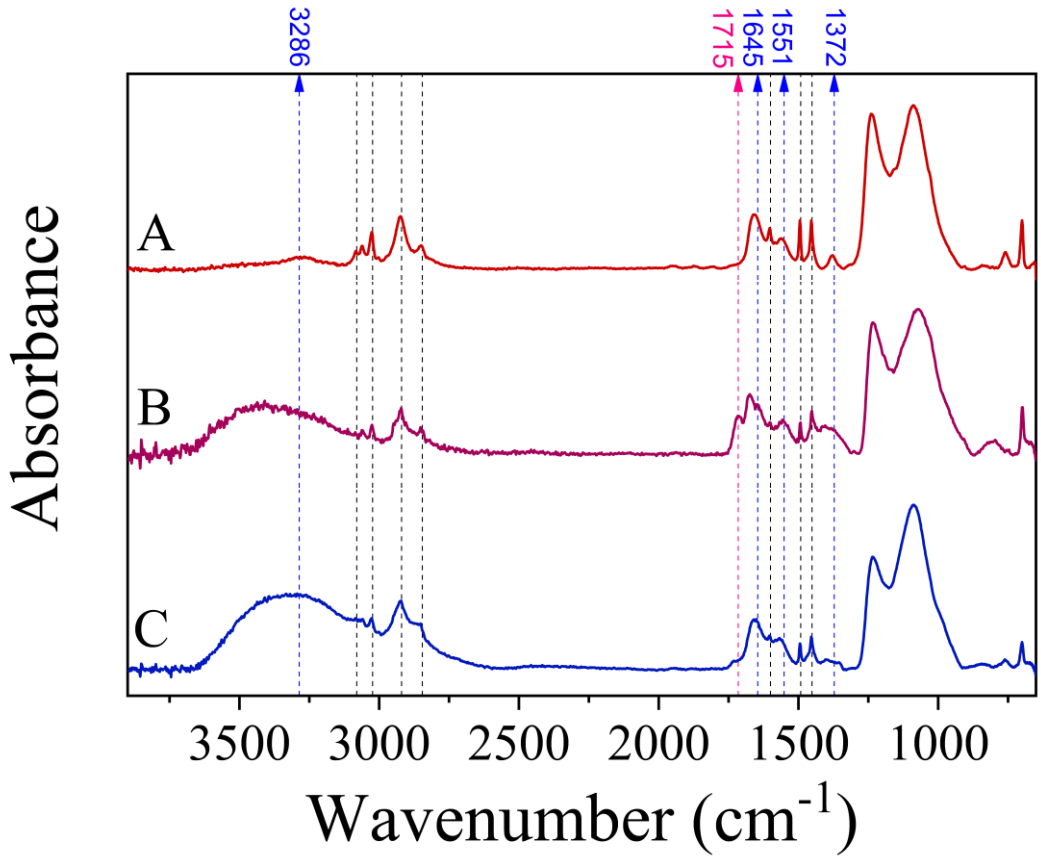

Figure 3. FTIR spectra of (A) PS-PAMAM, (B) GA-PS-PAMAM, and (C) AOX/PS-PAMAM ESNFs.

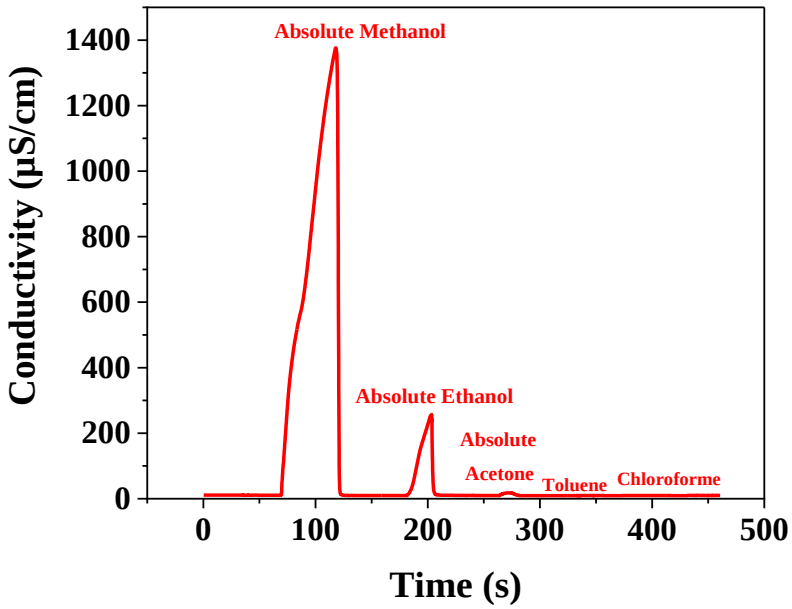

Figure 4. Detection of gas-phase concentrations above the pure liquid phase of MeOH, acetone, chloroform, ethanol, and toluene.

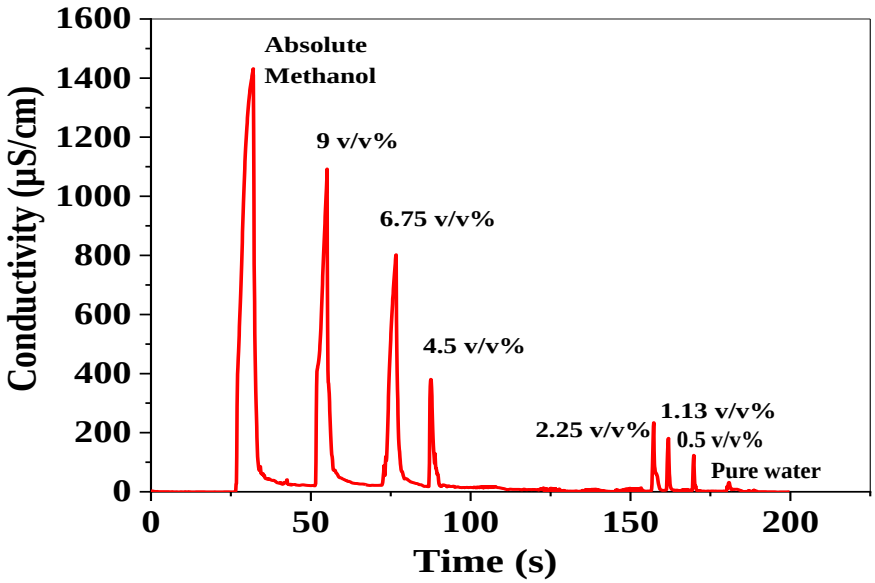

Figure 5. Detection of gas-phase concentration above different MeOH /water solutions with the MeOH sensor.

Table 1. Comparison of the analytical performances of conductometric MeOH sensors based on different materials.

Sensitive materials	Working Temperature	Response time (s)	Dynamic range (ppm)	Detection limit (ppm)	Ref.
Graphene oxide/polyindole	26 °C ± 1 °C	7	1.14 – 11.36	0.15	[26]
Pt doped SnO_2 nanoparticles	22 °C	10	0.13 − 5	0.13	[27]
TiO_2 nanotubes	RT	30	100 − 300	100	[28]
Tin dioxide doped cadmium sulfide	360 °C	−	0 − 6	0.9	[29]
Chitosan-NiPc film	25 °C	31	$700 - 10^5$	700	[30]
PVC-NiPc nanofibers	25 °C	13	$15 - 1.1x10^5$	15	[31]
AOX/PAMAM-PS-ESFs	25 °C	13	$100 - 10^5$	100	This work

Supplementary information

A conductometric enzymatic methanol sensor based on polystyrene - PAMAM dendritic polymer electrospun nanofibers

Pouyan Razmshoar[1,2], Anis Madaci[2], Fatma Besbes[2,3], Rym Mlika[3], S. Hajir Bahrami[1], Mohammad Rabiee[4], Marie Martin[2], Abdelhamid Errachid[2], Nicole Jaffrezic-Renault[2*]

1. Textile Engineering Department, Amirkabir University of Technology (Tehran Polytechnic), Tehran, Iran

2. University of Lyon, Institute of Analytical Sciences, UMR 5280, CNRS, F-69100, Villeurbanne, France

3. University of Monastir, Laboratory of Interfaces and Advanced Materials, Faculty of Science of Monastir, 5019 Monastir, Tunisia

4. Biomedical Engineering Department, Amirkabir University of Technology (Tehran Polytechnic), Tehran, Iran

Corresponding authors: Nicole Jaffrezic-Renault, nicole.jaffrezic@univ-lyon1.fr

Reagents and Solutions

Polystyrene (PS, MW = 192,000 g/mol) and N,N-dimethylformamide (DMF) (purity 99.9%) were purchased from Sigma-Aldrich. Poly(amidoamine) dendritic polymer equivalent to the second generation of poly(amidoamine) dendrimer (PAMAM) was provided by the Delta-Innovative Company, Poland. Alcohol Oxidase (AOX) from *Pichia pastoris* (10-40 units/mg protein), Bovine serum albumin (BSA) (96%), glutaraldehyde (GA), phosphate buffer saline (PBS) tablets, methanol (MeOH) (99.5%), ethanol (99.5%), acetone (99.5%), chloroform (99.5%), toluene (99.5%) were purchased from Sigma Aldrich. Ultra-pure water (UPW) (resistivity >18 MΩ cm) was produced by the ELGA System.

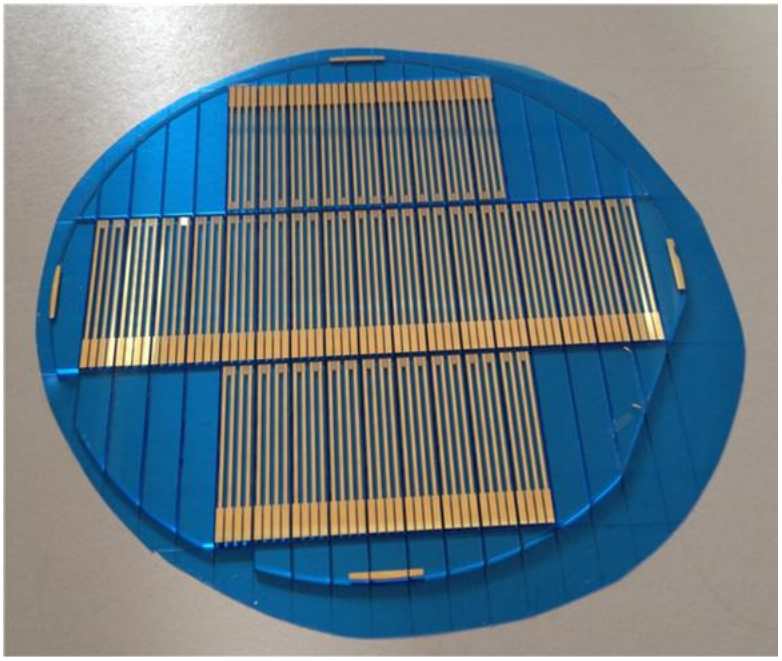

Figure S1. The glass wafer is covered with interdigital electrodes cut into pairs and supported on a blue film

Characterizations

Field emission scanning electron microscopy (FE-SEM, MIRA3 TESCAN) was used to characterize the morphology of ESNFs. Using the ImageJ analysis program, the average diameters and diameter distributions of ESFs were calculated from FE-SEM images by randomly picking 100 fibers from each of the ESNFs mats.

The surface chemical composition of ESNFs during methanol sensor preparation was characterized by Fourier Transform-Infrared (FTIR) using a NEXUS spectrophotometer (Nicolet-Thermo Fisher, UK) for 256 scans at a resolution of 4 cm^{-1}. The spectra were recorded in attenuated total reflectance (ATR) mode using a Thunder dome (Spectratech) accessory containing a germanium crystal with a mono reflection at 45°.

Table S1. Equilibrium gas-phase concentrations above an aqueous MeOH solution at 25 °C according to Henry's law constant given by Snider et al. [1] and Eq. (1) given by Sander [2].

Concentration of MeOH in the aqueous phase(M)	Concentration of MeOH in the gas phase(v/v%)
2.48	1.13
4.95	2.25
9.9	4.5
14.85	6.75
19.8	9
25.75	11.25

582

583

584

585 **Table S2.** Equilibrium gas-phase concentrations above an aqueous ethanol solution at 25 °C according

586 to Henry's law constant given by Snider et al. [1] and Eq. (1) given by Sander [2].

Concentration of ethanol in the aqueous phase(M)	Concentration of ethanol in the gas phase(v/v%)
1.71	0.90
3.41	1.79
6.82	3.58
10.23	5.37
13.64	7.16
17.15	9.02

587

588

589 **Table S3** Equilibrium gas-phase concentrations above an aqueous acetone solution at 25 $°C$ according

590 to Henry's law constant given by Snider et al. [1] and Eq (1). given by Sander [2].

Concentration of acetone in the aqueous phase(M)	Concentration of acetone in the gas phase(v/v%)

1.35	5.63
2.7	11.26
5.4	22.52
8.1	33.78
10.8	45.04
13.51	55.86

591

592

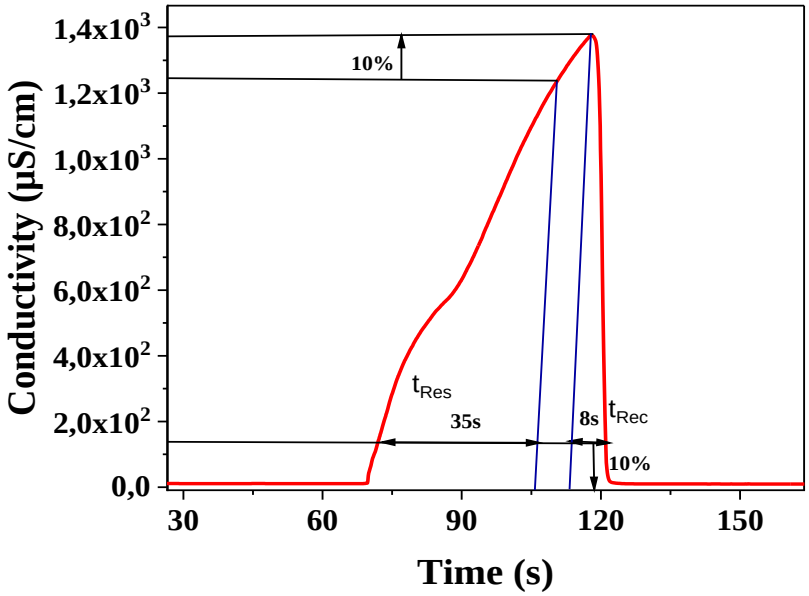

593

594 **Figure S2.** Measurements of the response time (t_{Res}) and recovery time (t_{Rec}) on the real-time

595 registration of the MeOH sensor signal for absolute methanol.

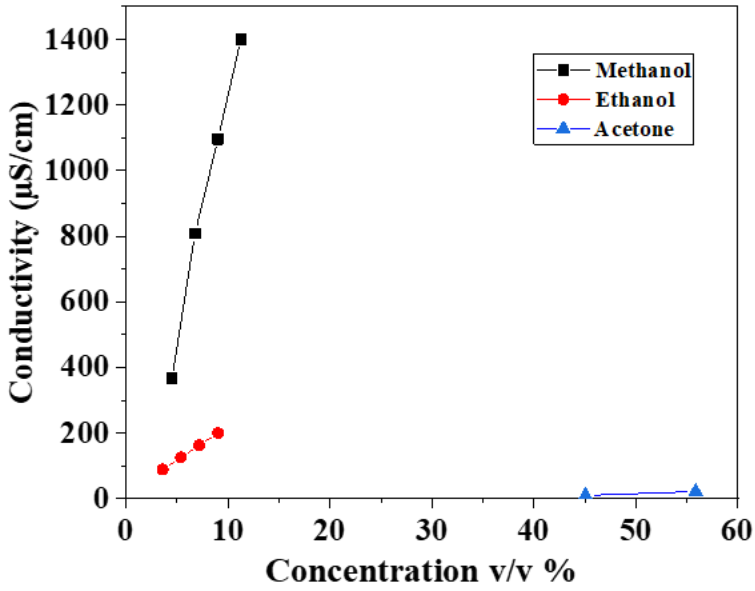

596

597 **Figure S3.** Calibration curves of MeOH, ethanol, and acetone in the gas phase of the AOX/PAMAM-
598 PS-ESNFs-based sensor. The size of the point is equal to the standard deviation.

599

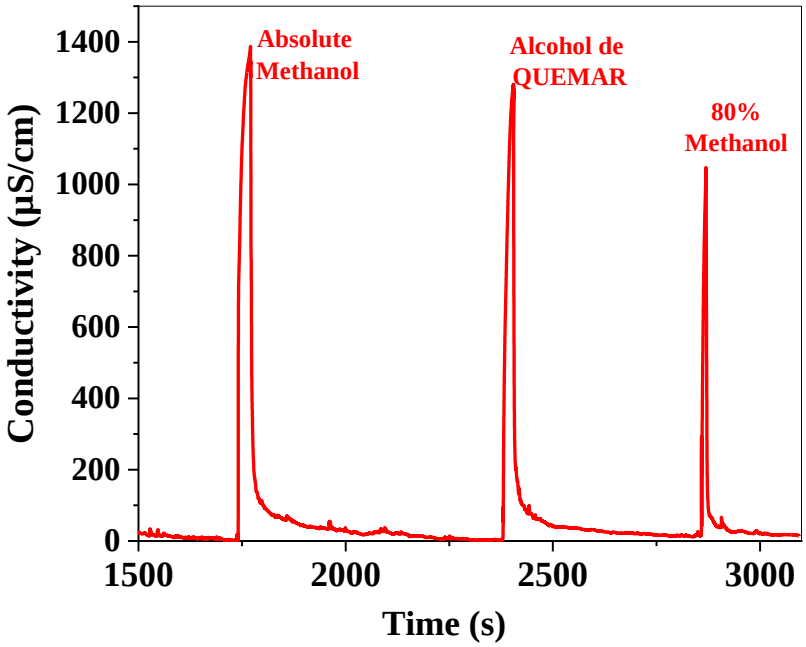

600

601 **Figure S4.** Detection of gas-phase concentration for different MeOH /water solutions and for the
602 rubbing alcohol with the AOX/PS-PAMAM-NFs.

603

References

[1] J.R. Snider, G.A. Dawson, Tropospheric light alcohols, carbonyls, and acetonitrile: Concentrations in the southwestern United States and Henry's law data, J. Geophys. Res. Atmos. 90 (1985) 3797–3805.

[2] R. Sander, Compilation of Henry's law constants for inorganic and organic species of potential importance in environmental chemistry, (1999).